Available online at www.sciencedirect.com

ScienceDirect

Energy Procedia 133 (2017) 312–326

Energy Procedia

www.elsevier.com/locate/procedia

Climamed 2017 – Mediterranean Conference of HVAC; Historical buildings retrofit in the Mediterranean area, 12-13 May 2017, Matera, Italy

Experimental and numerical investigation of the effects of wind exposure on historical towns

Fausto Arpino[a]*, Assunta Pelliccio[a], Gino Cortellessa[a], Andrea Frattolillo[b], Manuel Caschera[a]

[a]*Università degli Studi di Cassino e del Lazio Meridionale, via G. Di Biasio 43, Cassino 03043, Italy*
[b]*Università di Cagliari, via Marengo 2, Cagliari 09123, Italy*

Abstract

The Italian territory has a particularly rich cultural landscape, being composed of about 20.000 historic towns and villages, identified as "minor" only because of their relatively small dimension in comparison with the large cities. Many of these urban centers, especially in the southern Lazio, have not undergone the dynamic housing transformation, typical of other old towns, such as abandonment, replacement of the inhabitants with the inclusion of new social classes, or reuse of all or part for tourist-commercial purpose. It would seem that they have retained a "modus vivendi" antinomical of the non-places of contemporary cities, preserving a high social quality of aggregative life within urban arrangements characterized by a strong aesthetic identity. However, most of them are suffering significant degradation due to intrinsic reasons, such as the characteristics of the materials and the quality of construction, or external anthropogenic or environmental factors, such as, respectively, the lack of maintenance, humidity, solar irradiation and wind exposure. Often, the impact of these factors is compounded by the geographical position where these urban centers are located. In fact, many settlements arose and flourished in the Middle Ages, as result of the aggregation of minor architecture grown spontaneously. While, on one hand their original urban composition and the strong empathetic relationship with the natural environment represent an indubitable aesthetic value, they also are among the factors of major vulnerability. Frequently, the degradation of buildings facades has to be sought in the planimetric morphology of roads, forming street canyons where powerful wind channels are conveyed. Alveolization of natural stones or detachment of plaster are triggered by the erosive capacity of the wind enhanced by the development of mold and plants induced by the detainment of water and the low solar irradiation. The analysis of the environmental context is a fundamental step for the preservation of the historic buildings and for the whole project of restoration. In the present research this study is performed on a village (Borgo San Rocco) located in the southern Lazio. In particular, in the present paper the authors present the results of a wider research activity aimed at

* Corresponding author. Tel.: +39 0776 299 4324
E-mail address: f.arpino@unicas.it

Peer-review under responsibility of the scientific committee of the Climamed 2017 – Mediterranean Conference of HVAC; Historical buildings retrofit in the Mediterranean area
10.1016/j.egypro.2017.09.394

experimentally and numerically investigate historic buildings degradation due to wind exposure. The air velocity field and the viscous stresses in correspondence of the building walls of the Borgo San Rocco village have been numerically investigated by means of modern Computational Fluid Dynamics (CFD) techniques. Validation of the numerical results is obviously crucial. Velocity field, Reynolds stresses and wall viscous stresses significantly depend on the basic assumptions employed and on the turbulence mathematical modelling approach adopted. In order to validate the employed numerical tool a scaled model of part of the Borgo San Rocco Village has been realized with a 3D printer and the air velocity field about the model has been experimentally investigated in the wind tunnel available at the Laboratory of Industrial Measurements (LaMI) of the University of Cassino employing the Particle Image Velocimetry (PIV). A proper uncertainty analysis has been conducted to evaluate the measurement uncertainty affecting experiments. Measurements conducted at the LaMI have been numerically reproduced in order to validate the adopted CFD tool. The validated model will be applied to the simulation of the full-size Borgo San Rocco village in order to analytically correlate buildings degradation to local wind velocity and wall viscous stresses.

Peer-review under responsibility of the scientific committee of the Climamed 2017 – Mediterranean Conference of HVAC; Historical buildings retrofit in the Mediterranean area

Keywords: historical town; degradation; wind exposure; Particle Image Velocimetry (PIV); experimental; wind tunnel.

1. Introduction

In recent years, the preservation of the historic buildings heritage faces increasingly with the concept of environmental sustainability, intended as the process of social, architectural and urban renovation of villages or small and medium historical towns. The interest on these villages stems from the awareness of their modernity, given by the high quality of social life and by their aesthetic value.

Italy includes about twenty thousand small historic towns that, as for instance happens in Southern Lazio, have not lived the abandonment, replacement of inhabitants with new social classes, or the re-adaptation for touristic and commercial purposes typical of other situations. It would seem, in fact, that they represent antinomic symbols with respect to the modus vivendi of commercial centers or places lacking cultural and historical identity, i.e. the "non-places" of contemporary cities defined by Augee (Aguè, Marc, 1992).

The aesthetic value of these towns often comes from the strong empathetic relationship with the surrounding natural environment, that contributes to define their morphology and position and more often determines the use of specific and constructive techniques.

Grown in the Middle Ages as assemblies of poor houses, the beauty of these places is now given firstly by their urban composition that, following the topography of the area, complies tightly with the surrounding environment and then by the requirements for the environmental sustainability: their specificities for instance, are the use of masonry walls made of local stones enables to control the internal microclimatic factors such as temperature and humidity; the close conformation of the urban plant and the optimal sun orientation serves also to protect the towns from very heat and cold climate, exploiting as much as possible the benefits of passive heating; the orientation with regard to the prevailing wind direction, the color of the external facades and floor, are often designed to reduce the solar heat accumulation and enhance the light reflection; these are just few of the many possible environmental factors connected with the location of historic centers (Pelliccio, 2016).

With these specificities, the small historic towns respond well to social and environmental quality requirements, increasingly demanded by the contemporary society and are thus increasingly attractive from the viewpoint of the urban settlement. However, many of these towns presently live a significant degradation of their condition because of intrinsic phenomena, such as those connected with the degradation of the characteristics of materials, sometimes amplified by poor quality of construction, or external causes such as the lack of maintenance, humidity, solar radiation and wind exposure (Compagnon, 2004; Massimo et al., 2014). A semi-confined environment not prudently designed, with unsuitable microclimatic conditions (values of relative humidity near to saturation), can favor the generation of decay phenomena (Carcangiu et al., 2015) like salt crystallization, exfoliation or alveolization of natural stones or the detachment of plaster on the buildings facades of the stone with devastating effect for porous structures triggered by the erosive capacity of wind.

These factors are more relevant when the urban conformation forms long and narrow corridors, generally referred as street canyons, where the combination of water retention and low solar irradiation leads to the growth of mold and plants.

The above considerations lead to demand a "sustainable recovery", based on the concept of energy, faced with the complex systems of technical/urbanistic laws and guidelines for restoration: in the frequent case of protected buildings, it is necessary on one side to preserve their historical, aesthetic, textural and spatial characteristics, using compatible and reversible measures, on the other side to improve the energetic efficiency with deep and sometimes invasive modification and mitigate the degradation induced for example by the wind. The project of recovery must therefore make use of cognitive analyses, based not only on data regarding the structure, but moreover on the environmental context. The need to understand the dominant directions of wind and angles of incidence on the architectural surfaces is a key factor for the definition of a project of "environmental monument restoration".

Specifically, the analysis of the causes of degradation helps to choose more appropriate interventions of recovery: for instance, the inclusion, in urban context, of the curtain of trees, can reduce the wind impact on the facades of historical building, avoiding, in this way, to modify the shape of buildings, restricted by low.

In this paper, the authors present results of the experimentation implemented on a small village (St. Rocco) of Southern Lazio, based on the combination of a graphic/numerical and on-scale wind tunnel experiments to assess the effects of wind on the facades of buildings. The final goal of the work undertaken consists of the construction of a 3D real scale CDF tool, validated against wind tunnel experiments, able to predict facades viscous stress due to wind and to correlate them to observed degradation.

2. The “Borgo San Rocco” village

The case study of the village S. Rocco in Sothern of Lazio, best sums up the common issues of many small-medium Italian historical towns: due to its geometric, textural and territorial specificities, the degradation by wind on the facades of the buildings is very significant.

The origins of the village date back to the sixth century BC but it took its current shape in the first half of the seventeenth century, as evidenced by a bas-relief preserved in the Ducal Palace of Isola del Liri.

Fig. 1 Borgo San Rocco village: 3D graphic mode (left), southeast view (right top) and northwest view (right bottom).

The two building aggregates, which face each other between the Liri River and the foothills of Mount San Casto, present variable height. Buildings are composed by two to four floors, with a maximum height of 12 meters, and present a construction type load-bearing masonry. In particular, the device wall is uneven, consisting of mortar and calcareous rocks and clad of simple plaster (Fig. 1).

The homogeneity of the external composition contrasts with the interior which is rather uneven, with types of horizontal elements turned in the wooden floors, brick and cement, mixed etc. The vertical connecting elements (stairs) for all buildings are located in a longitudinal position. The coverage plan is a gable roof composed by wooden trusses, with the exception of the end buildings with a pavilion roof.

The urban layout of the village, oriented N.N.O., is similar to a street canyon. The longitudinal extension is 146 meters and the cross section instead varies from a minimum of 4 meters up to 11 meters.

The asymmetry of heights of buildings, does not allows to classify this urban core univocally as one family of "street canyons": because of the heights of the buildings on both sides are the same along the transverse section, the assessment of the section shape ratio H/W (H = height of the building; W = width of the road) in the point of minimum width of the street (10.9/4.0≃2.7) defines the village as a deep canyon. In the section that has the greatest width of the road, the village is presented instead as a regular canyon since the ratio between the maximum width point with the highest building worth (11.7/11.0≃1) while with the lower building worth (8.6/11.0≃0.8) (see Fig. 2). Furthermore, if the section shape ratio is rated in the media section of the heights on both sides with the minimum width of the road (9.7/4.0≃2.4) emerges even more that urban core presents the conformation at times as deep canyons and at times with a regular canyon.

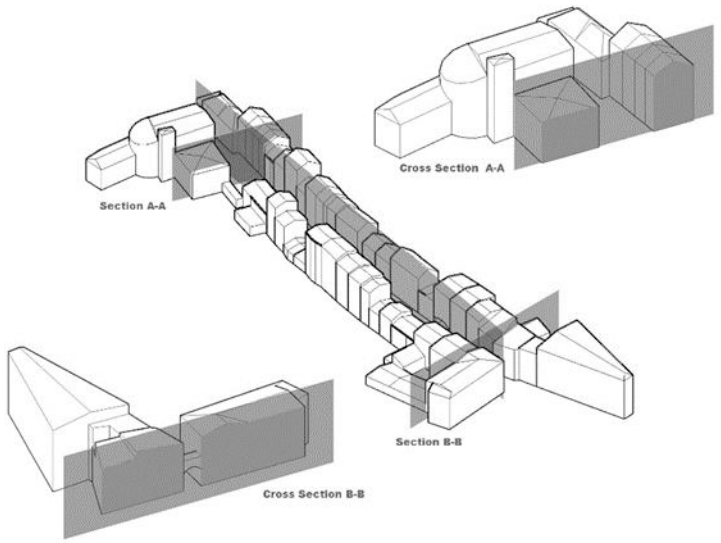

Fig. 2 3D graphic model of the Borgo San Rocco village: analysis of different sections aspect ratio.

3. On-scale experimental investigations

Computational Fluid Dynamic (CFD) technique (Arpino et al., 2016, 2015, 2013a, 2010a, 2010b; Arpino and Massarotti, 2009), if properly validated, represents a very useful support to measurements, reducing the number of experiments and so the costs. Beside, since results from numerical investigations depends on the employed turbulence modeling strategy, a comparison with experiments also allows to assess the performance of different turbulence models (H. K. Versteeg and W. Malalasekera, 1995; O. C. Zienkiewicz and R. L. Taylor, 2000; T. J. Chung, 2002; Tuncer Cebeci, 2004). Unfortunately, it is extremely difficult to collect on-field experimental data that can be used to validate CFD results since: i) Boundary Conditions (BCs) in most of the cases are not measurable and are difficult to be numerically reproduced; ii) BCs are not uniform and are time-dependent; iii) wind velocity measurements are possible just in specified locations in the space, usually not sufficient for a proper numerical validation; iv) on-field measurements can be affected by a significant measurement uncertainty, etc.

In order to experimentally validate CFD results about the air velocity in correspondence of the Borgo San Rocco village, a 1:200 on-scale model of part of the village has been realized using a 3D printer and has been experimentally investigated in the wind tunnel of the Laboratory of Industrial Measurements (LaMI) of the University of Cassino and Southern Lazio (Italy) (see Fig. 3).

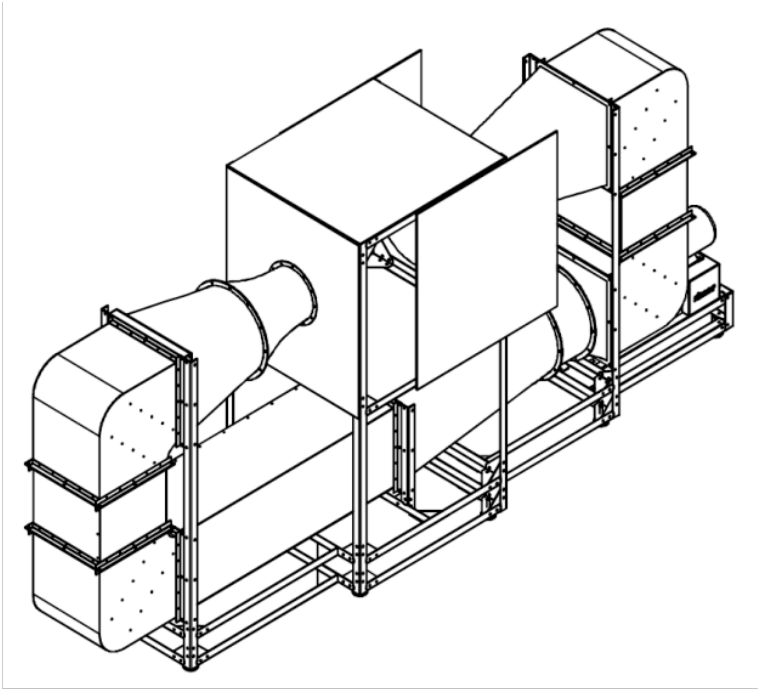

Fig. 3 Wind tunnel available at the Laboratory of Industrial Measurements (LaMI) of the University of Cassino.

The wind tunnel is located in a 150 m^3 room equipped with an ordinary mechanical ventilation system (air exchange rate equal to 0.3 h^{-1}), able to guarantee constant thermo-hygrometric conditions: in particular, temperature and humidity were kept constant at 20 ± 2 °C and 50 ± 5% RH, respectively. The wind tunnel of the LaMI consists of an inlet nozzle with a 16:1 contraction ratio, honeycombs type flow conditioners, vortex generators, a flow establishment section, a test section, anti-swirl devices, composed by honeycombs and grids, and a squirrel-cage centrifugal fan. A Direct Current (DC) electric motor with a thyristor type control system is able to push the air in correspondence of the test-section up to a speed of 25 m/s. The test chamber is 1.0 m high, 1.5 m wide and 0.4 m long, following a 7.5 m long development section just downstream of the boundary layer stimulation system.
The main dimensions of the on-scale model and wind direction imposed during measurements in the wind tunnel are available in Fig. 4. Air velocity measurements have been performed in correspondence of the dashed line in the "Top View" of Fig. 4. The model is constituted by two rows of buildings. The two rows of buildings constitute a street canyon geometry, that is a typical urban micro-environment formed when the street is flanked by buildings on both sides (P. Kumar et al., 2011; Scungio et al., 2013; Zhang et al., 2011). The most important geometric characteristic of a street canyon is its aspect ratio, which is the ratio between the street width W and the building height H. The maximum buildings height of the upstream row is equal to 83 mm, while the maximum buildings height of the downstream row is of 78 mm. The distance by the two buildings rows in correspondence of the measuring section is equal to 28mm, and the street canyon aspect ratio is of about 0.35.
The aim of experiments consists of producing a known, uniform and as steady as possible air flow in the measuring section. As a consequence, the experiments can be numerically reproduced and, comparing CFD results with experimental data, it is possible from one hand to select the most suitable turbulence model for the problem under investigation and, on the other hand, to validate numerical data.

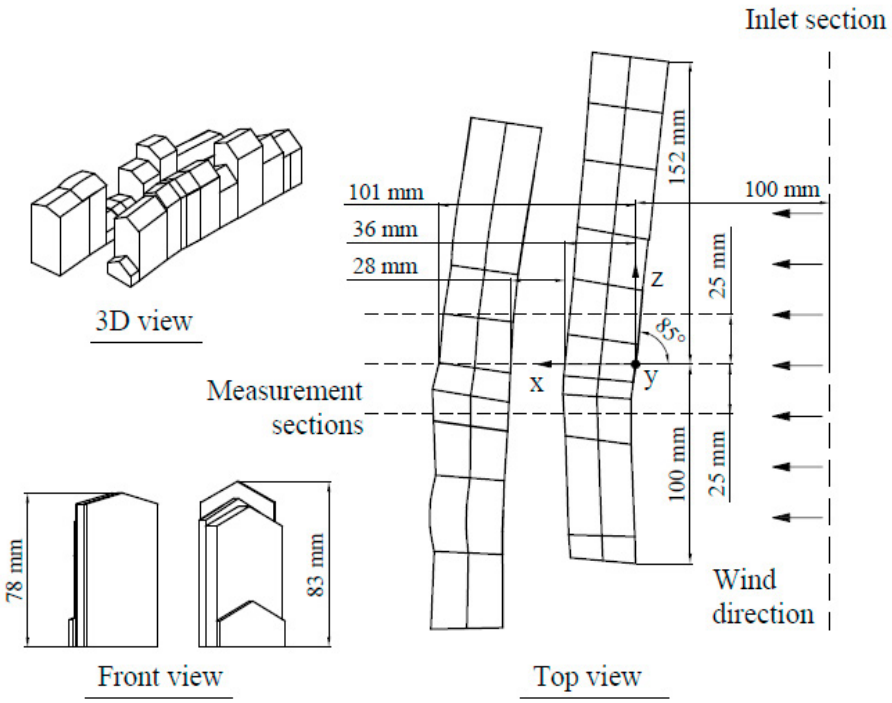

Fig. 4 1:200 scaled model of a part of the Borgo San Rocco village: main dimensions and wind.

It is important to notice that, for the given on-scale model dimensions and wind tunnel air velocity, the goal of the experiments conducted at the LaMI does not consists of reproducing the actual air velocity distribution in correspondence of the Borgo San Rocco village, but of producing reference experimental data, obtained in correspondence of an on-scale model of the village, useful for the selection of the turbulence model and the CFD validation. The selected turbulence model and CFD numerical tool could then be applied to the simulation of the full scale buildings of the Borgo San Rocco village, in order to predict viscous stresses in correspondence of the walls.
The velocity field around the on-scale model of the Borgo San Rocco village was characterized by means of the Particle Image Velocimetry (PIV) measurement equipment available at the LaMI. The PIV techniques allows the 2D reconstruction of the air velocity field in a non-intrusive way. Such technique is based on a simple principle: the flow is seeded by micron-sized particles and is illuminated twice by a laser light sheet in a very short time interval (Greated et al., 2002). The two images are obtained when the particles are illuminated, then the local velocity vectors reconstruction is obtained over different interrogation areas via cross-correlation method. As the time interval is short compared to the flow time scales, the PIV method delivers instantaneous velocity maps in a two-dimensional plane. Details about such non-intrusive measurement technique are available in the scientific literature (Lazar et al., 2010) and are not reported here for brevity.

3.1. Uncertainty analysis

An uncertainty analysis of the measured PIV data was provided on the basis of the well-known uncertainty propagation law. For brevity, only a brief description of the procedure is reported. The principle of the PIV measurement can be described by the following equation (T. Nishino et al., 2006):

$$w = \frac{\alpha(\Delta x)}{\Delta t} + \delta w \tag{1}$$

where $w(m\ s^{-1})$ is the velocity, Δx represents the pixel displacement between PIV image pairs, $\delta w\ (m\ s^{-1})$ takes

into account particle velocity lag from fluid acceleration together with three-dimensional effects on prospective of the velocity field, Δt represents the time interval between the two successive frames, $\alpha(m\,pixel^{-1})$ is the scaling magnification factor, representing the ration between the distance of the reference point l_R (mm) and its distance on the image plane L_R (px).

$$\alpha = \frac{l_R \cos(\theta)}{L_R} \cong \frac{l_R\left(1-\frac{\theta^2}{2}\right)}{L_R}\left(\frac{m}{pixels}\right) \tag{2}$$

where θ is a small angle between the light sheet and calibration board.
The uncertainty affecting PIV velocity measurements can be calculated by means of the following propagation law (Arpino et al., 2013b; Ficco et al., 2015; Heinonen et al., 2012; J. L. Bucher, 2004; R. C. Baker, 2000):

$$u_w = \sqrt{u_A^2 + \left(\frac{\partial w}{\partial \alpha}\right)^2 u_\alpha^2 + \left[\frac{\partial w}{\partial(\Delta x)}\right]^2 u_{\Delta x}^2 + \left[\frac{\partial w}{\partial(\Delta t)}\right]^2 u_{\Delta t}^2 + u_{\delta w}^2} \tag{3}$$

where u_w is the measured velocity standard uncertainty, u_A is the type A uncertainty, that for the case under investigation was evaluated equal to 0.1 m/s, while u_α, $u_{\Delta x}$, $u_{\Delta t}$, $u_{\delta w}$ represent the standard uncertainties of difference influence parameters. The average velocity profiles are obtained from a number of acquisitions equal to 500. As a consequence, in the present work uncertainty source related to Δt was considered negligible. As a result of the uncertainty analysis, it was found that the maximum composed velocity uncertainty, calculated assuming a coverage factor k=2 (confidence level 95%), was equal to 0.42 m/s, corresponding to 2.8 % of the free stream velocity, for the upstream acquisition zone, and 0.45 m/s, corresponding to 3.0 % of the free stream velocity.

3.2. Experimental results

Fig. 3 shows the on-scale model in the test chamber of the wind tunnel. The air moves from the left to the right, as indicated by the green arrows in the figure, while the laser light comes from the top of the test chamber allowing a 2D measurement of the velocity field. As indicated in Fig. 3, measurements have been conducted in three zones: upstream, canyon and downstream zone.

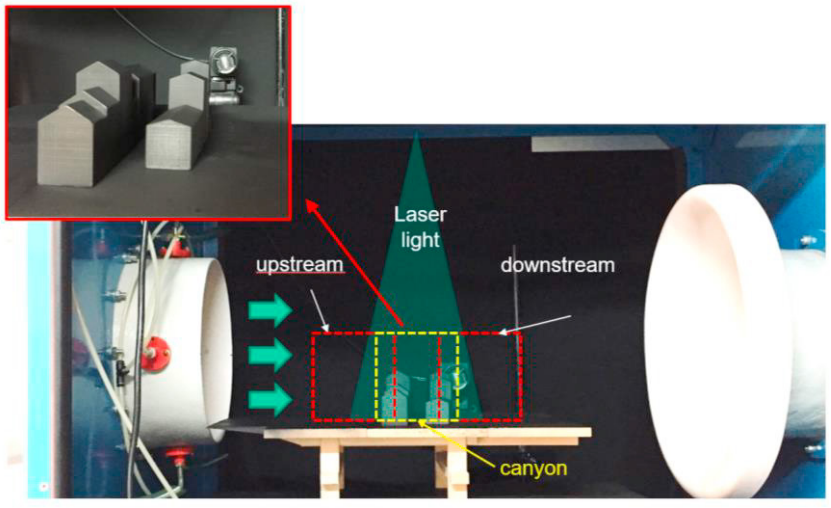

Fig. 5. scaled model of a part of the Borgo San Rocco village placed in the wind tunnel of the LaMI.

The main test parameters of the PIV measurements are listed in Table 1. The air flow velocity in the wind tunnel was set to 10 m/s and the experiments were conducted at a temperature of 20 °C. For each experiment 500 PIV image couples have been acquired with a sampling frequency of 7.25 Hz and the instantaneous velocity field has been reconstructed via standard cross-correlation technique (Greated et al., 2002). Derived turbulence quantities, such

Turbulent Kinetic Energy (TKE) and Reynolds stresses (H. K. Versteeg and W. Malalasekera, 1995; Scungio et al., 2013), have been computed and the 300 instantaneous velocity fields have been averaged in time.
Fig. 6 shows the time-averaged x-velocity component (left) and the x-velocity expanded uncertainty (right) obtained in correspondence of the canyon zone for an inlet air velocity of 10 m/s. The air velocity module inside the street canyon is lower than 5 m/s and a recirculating zone is observed upstream the first building in the wind direction. From the analysis of Fig. 6(b) it is possible to observe that the max value of the velocity uncertainty is about 0.4 m/s in proximity of the roof, where fluctuating component of the velocity is larger, while the lower uncertainty values are reached near the walls, where, as expected, viscous forces become predominant with respect to inertia forces.
Fig. 7 shows the x-velocity fluctuating component (left) and the turbulence kinetic energy (right) obtained in correspondence of the canyon for an inlet air velocity of 10 m/s. From the analysis of such figure is can be observed that the oscillating x-velocity component is larger in the wake generated by the top of the first row of buildings. As a consequence, the x-velocity uncertainty is larger in such zone since a larger type A contribution is obtained.

Table 1. Main test parameters of PIV measurements.

Target flow	Upstream zone	Canyon zone	Downstream zone
Measurement area	131 × 131 mm	132 × 132 mm	134 x 134 mm
Air temperature, T_{REF}	20 °C		
Calibration			
Distance of reference points, l_R	120 mm	120 mm	120mm
Distance of reference image, L_R	1874 pixels	1861 pixels	1829
Magnification factor, α	15.62 pixel/mm	15.51 pixel/mm	15.24 pixel/mm
Flow visualization			
Tracer generator	Fog Machine		
1-min average particles diameter (mode), d_p	1.2 μm		
Light source	Double pulse laser		
Max laser power	135 mJ at 532 nm		
Thickness of the laser light sheet	≅1.0 mm		
Time interval, Δt	80 μs		
Image detection			
Camera resolution	2048×2048 pixels		
Sampling frequency	7.25 Hz		
Distance from target, l_t	0.532 m	0.537 m	0.544 m
Prospective angle, θ	14.1 °	13.9°	14.1°
Data processing			
Pixel unit analysis	Cross correlation method		
Correlation area size	32 × 32 pixels		

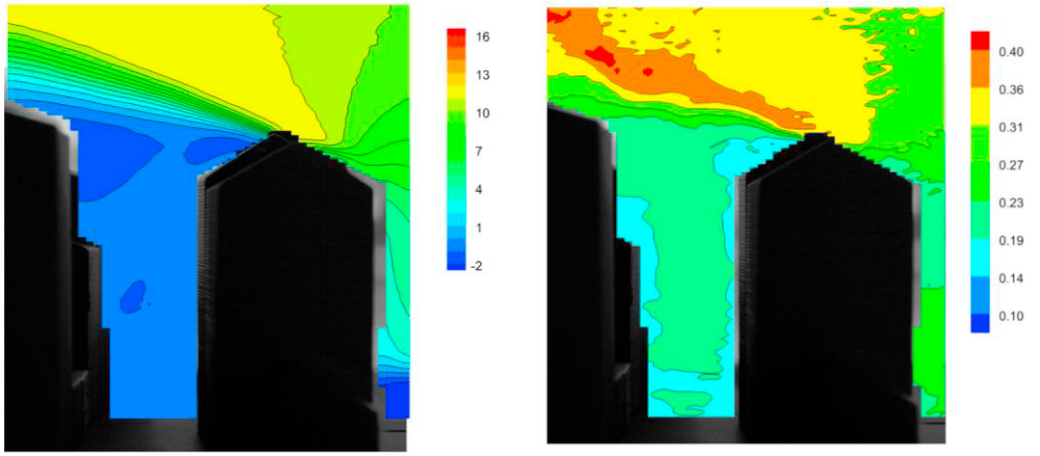

(a) (b)

Fig. 6 PIV measurements in the canyon zone for an inlet air velocity of 10 m/s: a) time-averaged x-velocity module field U(m/s); b) x-velocity expanded uncertainty (m/s), with a coverage factor k=2.

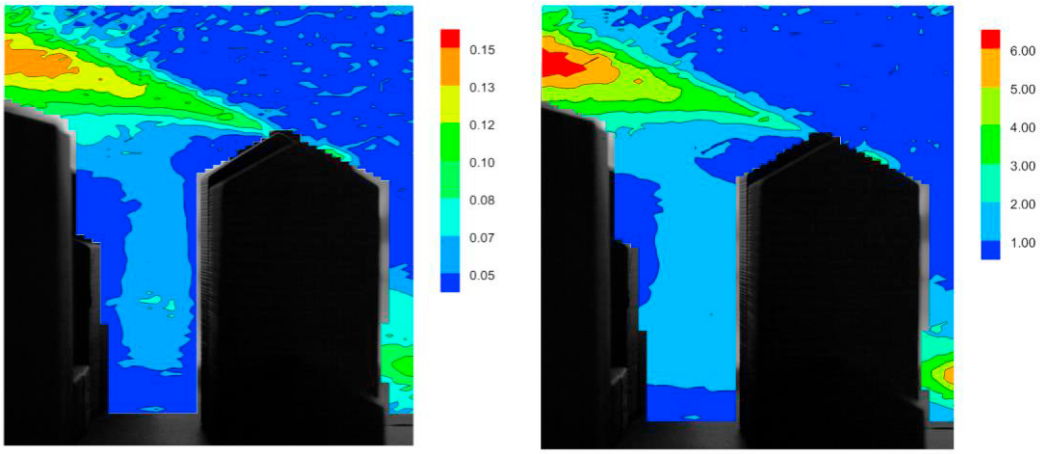

(a) (b)

Fig. 7 PIV measurements in the canyon zone for an inlet air velocity of 10 m/s: a) x-velocity fluctuating component u' (m/s); b) turbulence kinetic energy k (m^2/s^2).

4. Numerical investigations

Experiments were accompanied by numerical investigations that allowed a better understanding of local wind velocity and wall viscous stresses on the facades of buildings. Preliminary numerical investigations have been conducted employing the finite volume based open source code OpenFoam®, under the following assumptions: steady state conditions, incompressible flow, constant and uniform thermo-physic properties of the air and constant and uniform temperature. Numerical simulations reproduced the on-scale experiments in the wind tunnel, with an air velocity of 10 m/s. Details about the governing equations, the computational domain, the model validation and the obtained results are reported in the following subsections.

4.1. Governing equations

The fluid velocity and pressure fields have been obtained by solving the well-known mass and momentum conservation equations (Arpino et al., 2014, 2015, 2016; M. Scungio et al., 2015; Massarotti et al., 2016), not reported here for brevity. Turbulence has been modelled using the Reynolds Averaged Navier Stokes (RANS) approach and employing the Realizable $k-\epsilon$ model. With respect to the standard $k-\epsilon$ model, the Realizable $k-\epsilon$ model contains a new formulation for the turbulent viscosity and a new transport equation for the dissipation rate, ε, derived from an exact equation for the transport of the mean-square vorticity fluctuation. Besides, it introduces a variable Cμ instead of constant, ensuring superior performance for flows involving rotation, boundary layers under strong adverse pressure gradients, separation, and recirculation (H. K. Versteeg and W. Malalasekera, 1995). Results obtained by employing the turbulence model have been compared to experiments in order to analyzed the accuracy and the reliability of the selected model for the description of the problem under investigation. In the following, the Partial Differential Equations (PDEs) solved for the Realizable k- ε turbulence model are briefly reported.

Turbulent kinetic energy k:

$$\frac{\partial(\rho u_j k)}{\partial x_j} = \frac{\partial}{\partial x_j}\left[\left(\mu + \frac{\mu_T}{\sigma_k}\right)\frac{\partial k}{\partial x_j}\right] + G_k - \rho\varepsilon - Y_M + S_k \tag{4}$$

Turbulent dissipation ε:

$$\frac{\partial(\rho u_j \epsilon)}{\partial x_j} = \frac{\partial}{\partial x_j}\left[\left(\mu + \frac{\mu_T}{\sigma_\varepsilon}\right)\frac{\partial \varepsilon}{\partial x_j}\right] + \rho C_1 S\epsilon - \frac{\rho C_2(\epsilon^2)}{k+\sqrt{(\nu\epsilon)}} + \frac{C_{1\epsilon}\epsilon}{k} C_{3\epsilon} G_b + S_\epsilon \tag{5}$$

where:

$$C_1 = \max\left(0.43, \frac{\eta}{\eta+5}\right), \qquad \eta = S\left(\frac{k}{\epsilon}\right), \qquad S = \sqrt{2S_{ij}S_{ij}} \tag{6}$$

In the above equations, the term G_k represents the generation of k related to mean velocity gradients, S_k and S_ϵ are source term of turbulence kinetic energy and turbulent dissipation rate, respectively, C_1 and $C_{1\epsilon}$ are constant, σ_k and σ_ϵ represent the turbulent Prandtl numbers for k and ϵ. Further details about the Realizable $k-\epsilon$ turbulence mode are available in the scientific literature (Kumar, 2014) and are not reported here for brevity.

4.2. Computational domain and boundary conditions.

Information about the computational domain are available in Fig. 4. In particular, the computational domain extends for 0.4 m in the x and z directions and 0.2 m in the y direction. The inlet section is located at a distance of 0.1 m from the first row of buildings. The vertical profile of x-velocity, y-velocity and turbulent kinetic energy measured in correspondence of the inlet section employing the PIV technique are imposed as Dirichlet boundary condition for numerical investigations. Turbulence dissipation rate value at the inlet section is calculated employing the turbulent model correlations. A zero pressure boundary condition is imposed at the outlet, located at a distance of 0.4 m from the inlet section in the x-direction. A wall boundary condition is imposed in correspondence of the buildings facades and bottom side of the domain, while a symmetry boundary condition is imposed in correspondence of the remaining sides. Fig. 8 shows the computational grid employed for computation that has been realized using the commercial software Pointwise® and is composed by 5664742 tetrahedral cells, is refined near the walls, as highlighted in the enlargement, to properly capture the gradients of the quantities of interest in correspondence of the boundary layers. The minimum mesh size is equal to 0.0005 m, while the maximum size is equal to 0.02 m, ensuring a y^+ value of about 5 in correspondence of the buildings facades ad of about 15 in correspondence of the roof top, where the air velocity is maximum.

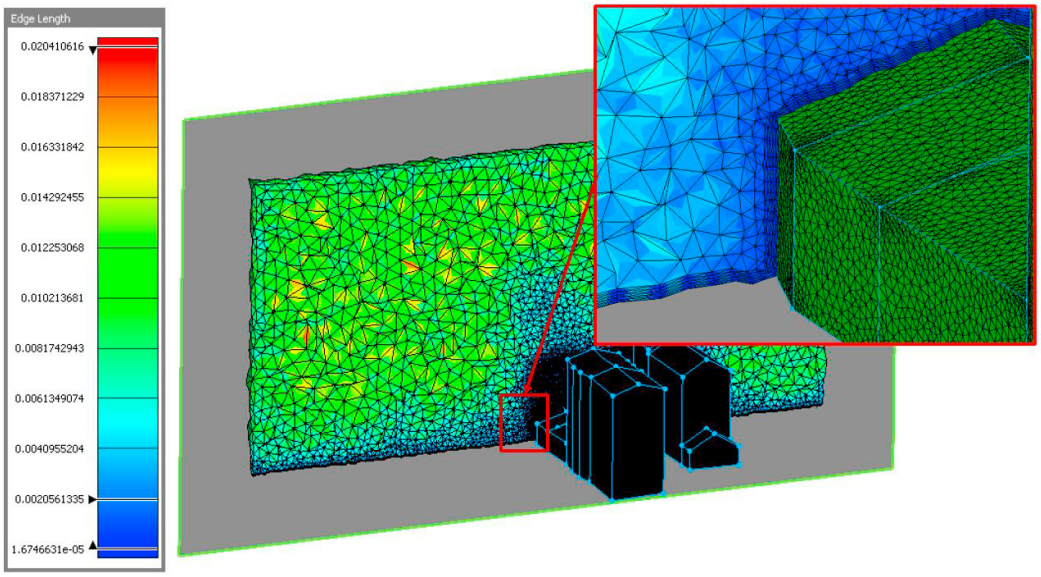

Fig. 8 Computational grid composed by 5664742 cells with an enlargement near the walls.

4.3. Results and validation

Numerical simulations reproduced the wind tunnel experiments for an air velocity of 10 m/s. Fig. 9 shows the horizontal velocity contours numerically obtained in correspondence of the measurement plane during experiments. From the analysis of such figure it can be clearly evidenced a recirculation zone in the canyon region and downstream the second row of buildings in the x-direction, where negative values of the x-velocity are obtained ($\cong -2\ m/s$). As expected, the maximum x-velocity values are obtained above the roof ($\cong 16\ m/s$) where the impact of the surrounding air becomes dominant.

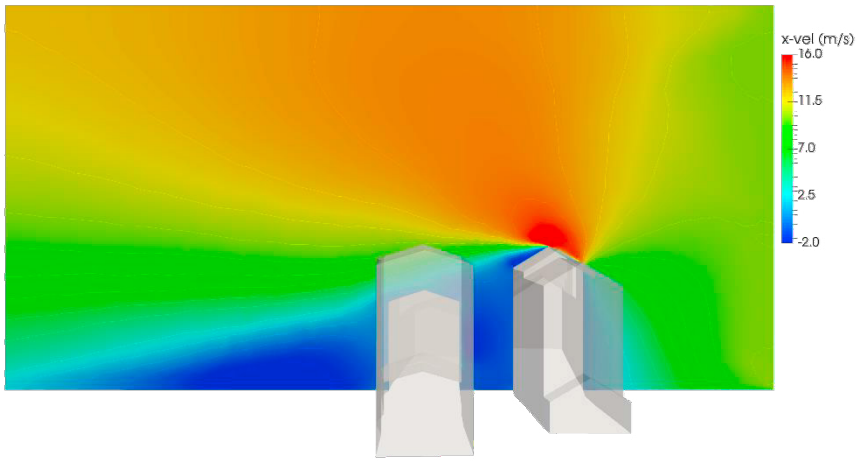

Fig. 9 Horizontal velocity field obtained in correspondence of the measurement section. Wind velocity equal to 10 m/s.

Results from numerical investigations have been validated against data collected during experiments. Fig. 10 and Fig. 11 show the comparison between numerical results and PIV measurements for x=41 mm and x=50 mm, respectively, in terms of horizontal component of the velocity. Errors bars in the figures are representative of the

measurement uncertainty and the comparison is performed in terms of data compatibility. These figures clearly show that a good agreement is obtained between preliminary numerical results and measurements. In particular, computations are able to correctly capture the boundary layer in correspondence of the bottom wall (y=0), while some discrepancies are evidenced in the free stream zone, where numerical results tend to overestimate experiments. This behavior is anyway expected from RANS turbulence models when fluid flow problems that exhibit adverse pressure gradient are investigated, suggesting that the performance of different RANS models and Large Eddy Simulation (LES) approach must be investigated.

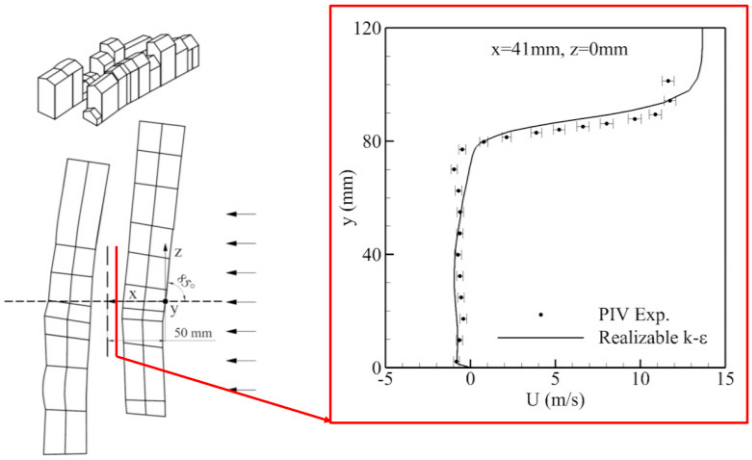

Fig. 10 Comparison between experimental and numerical results: velocity magnitude profile (m/s) as a function of the y coordinate (mm) obtained in correspondence of a x-coordinate equal to 41mm.

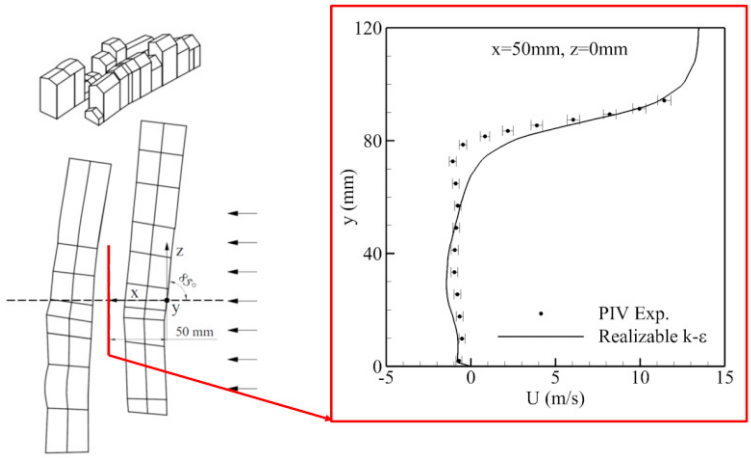

Fig. 11 Comparison between experimental and numerical results: velocity magnitude profile (m/s) as a function of the y coordinate (mm) obtained in correspondence of a x-coordinate equal to 50 mm.

Fig. 12 shows the calculate y^+ value in correspondence of the solid walls of the buildings. As expected the y^+ value increases in correspondence of the top of the buildings, where the air velocity increases, while it is minimum where a recirculation zone is present. The maximum y^+ value is not larger than 15, that allows to proper capture the velocity gradient in correspondence of the boundary layer.

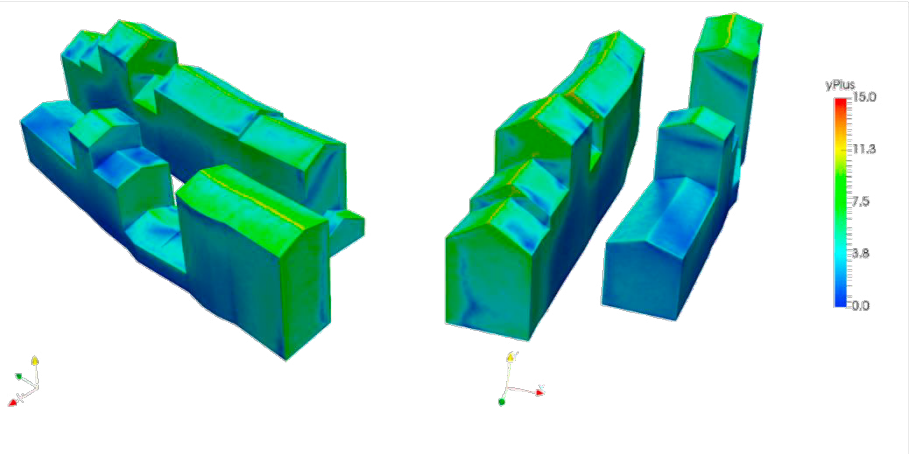

Fig. 12. Calculated y+ value in correspondence of the solid wall of buildings for an air velocity of 10 m/s.

Finally, Fig. 13 shows the calculates shear stresses in correspondence of solid walls of the buildings, obtained for and air velocity of 10 m/s. As expected, shear stresses are maximum in correspondence of the top of the first row of buildings. In fact, the first row of buildings behaves as a wind screen for the second row of buildings. Besides, large shear stresses are present in the area between the tallest and the lower buildings, since an air flow acceleration is observed.

It is important to point out that this results are obtained on the on-scale model and that, as a future development, will be applied to the full scale case, evidencing the zones of the buildings walls where more significant effects due to wind exposure are expected. Such numerical previsions, is properly confirmed by on-place observed degradation by wind exposure, will allow the construction of a numerical tool that could be useful for defining the necessary actions to preserve historical heritage.

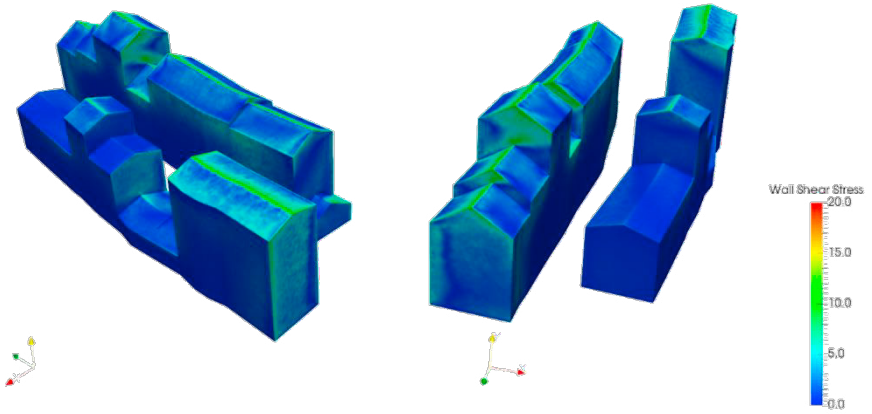

Fig. 13 Wall shear stresses calculated in correspondence of the walls of the buildings for an air velocity of 10 m/s.

5. Conclusions

The social quality of life and the aesthetic value of small historical towns require the preservation of their built heritage. In fact, most of historical villages are suffering significant degradation due to intrinsic reasons, such as the characteristics of the materials and the quality of construction, or external anthropogenic or environmental factors, such as, respectively, the lack of maintenance, humidity, solar irradiation and wind exposure.

The aim of this work is to correlate air velocity field, viscous shear stresses and pressure distribution in correspondence of historical buildings to degradation phenomena due to wind exposure.

The phenomenon of wind action on buildings of the Borgo San Rocco village has been analyzed by means of experiments on a 1:200 on-scale model of a portion of the Borgo San Rocco village, conducted at the Laboratory of Industrial Measurements (LaMI) of the University of Cassino, employing the wind tunnel and Particle Image Velocimetry (PIV) technique. Besides, numerical investigations have been conducted by means of the modern Computational Fluid Dynamic (CFD) techniques, in order to reproduce the experiments conducted at the LaMI. Numerical investigations have been conducted employing the Realizable $k-\epsilon$ turbulence model.

A proper uncertainty analysis has been conducted on the PIV measurements and numerical results have been validated against experiments and the validated model has been employed to analyses the shear stresses in correspondence of the solid walls of the buildings.

As a future development, the performance of different turbulence model will be assessed (RANS, LES) and the CFD model will be applied to the simulation of the full scale Borgo San Rocco village in order to correlate local viscous stresses due to wind velocity field to local degradation of the buildings facades. If properly confirmed by on-place observed degradation by wind exposure, the proposed investigation approach will allow the construction of a numerical tool that could be useful for defining the necessary actions to preserve historical heritage.

References

Aguè, Marc. Non-Places. Introduction to an anthropology of supermodernity. London: Verso; 1992.

Pelliccio A. Cognitive analysis for historical towns: digital representation and computational simulation to investigate the effects of solar radiation and wind exposure. Bertocci Stefano, Bini Marco: The reasons of drawing, Rome: Gangemi; 2016.

Compagnon R. Solar and daylight availability in the urban fabric. Energy and Buildings 2004;36:321–8.

Massimo A, Dell'Isola M, Frattolillo A, Ficco G. Development of a geographical information system (GIS) for the integration of solar energy in the energy planning of a wide area. Sustainability (Switzerland) 2014;6:5730–44.

Carcangiu G, Casti M, Desogus G, Meloni P, Ricciu R. Microclimatic monitoring of a semi-confined archaeological site affected by salt crystallisation. Journal of Cultural Heritage 2015;16:113–8.

Arpino F, Carotenuto A, Ciccolella M, Cortellessa G, Massarotti N, Mauro A. Transient natural convection in partially porous vertical annuli. International Journal of Heat and Technology 2016;34:S512–8. doi:10.18280/ijht.34S245.

Arpino F, Cortellessa G, Frattolillo A. Experimental and numerical assessment of photovoltaic collectors performance dependence on frame size and installation technique. Solar Energy 2015;118:7–19. doi:10.1016/j.solener.2015.05.006.

Arpino F, Carotenuto A, Massarotti N, Mauro A. New solutions for axial flow convection in porous and partly porous cylindrical domains. International Journal of Heat and Mass Transfer 2013a;57:155–70.

Arpino F, Massarotti N, Mauro A. A stable explicit fractional step procedure for the solution of heat and fluid flow through interfaces between saturated porous media and free fluids in presence of high source terms. International Journal For Numerical Methods In Engineering 2010a;83:671–92.

Arpino F, Massarotti N, Mauro A. High rayleigh number laminar-free convection in cavities: New benchmark solutions. Numerical Heat Transfer, Part B: Fundamentals 2010b;58:73–97.

Arpino F, Massarotti N. Numerical simulation of mass and energy transport phenomena in solid oxide fuel cells. Energy 2009;34:2033–41.

H. K. Versteeg, W. Malalasekera. An introduction to computational fluid dynamics. The finite volume method. Essex, England: 1995.

O. C. Zienkiewicz, R. L. Taylor. The Finite Element Method, Vol 3, Fluid Dynamics. Oxford: Butterworth and Heinemann; 2000.

T. J. Chung. Computational Fluid Dynamics. Cambridge University Press; 2002.

Tuncer Cebeci. Turbulence Models and Their Application. Long Beach, California: Horizons Publishing Inc.; 2004.

P. Kumar, M. Ketzel, S. Vadoulakis, L. Pirjola, R. Britter. Dynamics and dispersion modelling of nanoparticles from road traffic in the urban atmospheric environment - A review. Journal of Aerosol Science 2011;42:580–603.

Scungio M, Arpino F, Stabile L, Buonanno G. Numerical simulation of ultrafine particle dispersion in urban street canyons with the spalart-allmaras turbulence model. Aerosol and Air Quality Research 2013;13:1423–37.

Zhang Y-W, Gu Z-L, Cheng Y, Lee S-C. Effect of real-time boundary wind conditions on the air flow and pollutant dispersion in an urban street canyon - Large eddy simulations. Atmospheric Environment 2011;45:3352–9.

Greated C, Cosgrove J, Buick J. Optical Methods for Data Processing in Heat and Fluid Flow. 2002.

Lazar E, DeBlauw B, Glumac N, Dutton C, Elliott G. A Practical Approach to PIV Uncertainty Analysis, Chicago, Illinois: 2010.

T. Nishino, H. Iwai, K. Suzuki. Comprehensive Numerical Modeling and Analysis of a Cell-Based Indirect Internal Reforming Tubular SOFC. Journal of Fuel Cell Science and Technology 2006;3:33–44.

Arpino F, Dell'Isola M, Maugeri D, Massarotti N, Mauro A. A new model for the analysis of operating conditions of micro-cogenerative SOFC units. International Journal of Hydrogen Energy 2013b;38:336–44.

Ficco G, Dell'Isola M, Vigo P, Celenza L. Uncertainty analysis of energy measurements in natural gas transmission networks. Flow Measurement and Instrumentation 2015;42:58–68. doi:10.1016/j.flowmeasinst.2015.01.006.

Heinonen M, Anagnostou M, Bell S, Stevens M, Benyon R, Bergerud RA, et al. Investigation of the Equivalence of National Dew-Point Temperature Realizations in the −50 °C to + 20 °C Range. International Journal of Thermophysics 2012;33:1422–37. doi:10.1007/s10765-011-0950-x.

J. L. Bucher. The metrology handbook, the measurement quality division, ASQ, 2004. 2004.

R. C. Baker. Flow Measurement Handbook - Industrial designs, operating principles, performance and applications. New York: Cambridge University Press; 2000.

Arpino F, Cortellessa G, Dell'Isola M, Massarotti N, Mauro A. High order explicit solutions for the transient natural convection of incompressible fluids in tall cavities. Numerical Heat Transfer; Part A: Applications 2014;66:839–62. doi:10.1080/10407782.2014.892389.

M. Scungio, F. Arpino, G. Cortellessa, G. Buonanno. Detached eddy simulation of turbulent flow in isolated street canyons of different aspect ratios. Atmospheric Pollution Research 2015;6:351–64.

Massarotti N, Ciccolella M, Cortellessa G, Mauro A. New benchmark solutions for transient natural convection in partially porous annuli. International Journal of Numerical Methods for Heat & Fluid Flow 2016;26:1187–225. doi:doi:10.1108/HFF-11-2015-0464.

Kumar A. Analysis of Heat Transfer and Fluid Flow in Different Shaped Roughness Elements on the Absorber Plate Solar Air Heater Duct. Energy Procedia 2014;57:2102–11. doi:10.1016/j.egypro.2014.10.176.